Proc. Natl. Acad. Sci. USA
Vol. 89, pp. 5167–5170, June 1992
Biochemistry

Solvent dielectric effects on protein dynamics

RHETT AFFLECK, CHARLES A. HAYNES, AND DOUGLAS S. CLARK*

Department of Chemical Engineering, University of California, Berkeley, CA 94720

Communicated by John M. Prausnitz, February 24, 1992 (received for review November 4, 1991)

ABSTRACT **Electron paramagnetic resonance (EPR) spectroscopy and molecular dynamics (MD) simulations were used to investigate the dynamics of α-chymotrypsin in solvents ranging in dielectric constant from 72 to 1.9. EPR measurements showed that motions in the vicinity of two spin-labeled amino acids (Met-192 and Ser-195) decreased dramatically with decreasing solvent dielectric constant, a trend consistent with changes in the electrostatic force between charged residues of the protein. EPR results and MD simulations revealed a very similar functional dependence between rates of motion in the protein and the dielectric constant of the bulk solvent; however, predicted motions of protein atoms were markedly faster than measured motions of the spin labels. MD calculations for dielectric constants of 5 and 72 showed the greatest differences near the outer surface of the protein. In general, at the lower dielectric constant many atoms of the protein move more slowly, and many of the slowest residues are near the exterior. These results suggest that altered dynamics may contribute to the unusual properties—e.g., modified stereoselectivities—of enzymes in nearly dry organic solvents.**

The dynamic nature of proteins has been revealed by a variety of experimental and theoretical techniques. Physical methods used to study protein dynamics include NMR spectroscopy (1), x-ray diffraction (2), inelastic neutron scattering (3), and time-domain reflectrometry (4). In addition, computer simulations, particularly molecular dynamics (MD) calculations, have disclosed high-frequency protein motions in fine detail (5, 6).

Motions in proteins are governed in part by electrostatic interactions. In fact, a growing body of experimental and theoretical evidence indicates that electrostatic forces are the dominant factor correlating protein structure and function (7–9). Attenuation of such forces by the solvent environment can be dramatic, particularly in solvent-accessible regions of proteins (4). The dielectric constant of the solvent should thus have a major influence on protein dynamics. However, the sensitivity of protein motions to large variations in solvent dielectric constant has not been carefully examined in previous studies. In this work, we focus on the role of electrostatic forces in determining the dependence of protein dynamics on the solvent environment.

Nonaqueous solvents, in which many enzymes exhibit good catalytic activity and enhanced thermal stability (10, 11), are emerging as versatile media for fundamental studies of enzyme structure and function (12). In particular, nearly anhydrous organic solvents enable studies of protein properties in low-dielectric environments. In this report, we compare the dynamics of α-chymotrypsin in solvents ranging in dielectric constant from 72 to 1.9. Motions in the vicinity of two amino acids—Met-192 and Ser-195—were probed by electron paramagnetic resonance (EPR) spectroscopy and the spin-labeling technique.

The publication costs of this article were defrayed in part by page charge payment. This article must therefore be hereby marked "*advertisement*" in accordance with 18 U.S.C. §1734 solely to indicate this fact.

In general, the EPR spectrum of a spin-labeled enzyme is very sensitive to the motion of the spin label. The spin label can be viewed as an uncharged extraneous side-chain residue of the protein, and responses of the neighboring protein to a change of environment (i.e., an increase in temperature or a change of solvent) will be manifested by the behavior of the spin label. For example, in studies of protein hydration, the EPR spectra of bound spin labels have reflected motions of the surrounding protein (13). Here we examine the correspondence between spin label motion and protein dynamics in greater detail by comparing the results of spectral simulations and MD calculations.

MATERIALS AND METHODS

The active-site region of α-chymotrypsin (type II; Sigma) was spin labeled in separate experiments with *N*-(1-oxyl-2,2,6,6-tetramethyl-4-piperidinyl)iodoacetamide (SL-1; obtained from Aldrich), which reacts exclusively with the thioether of Met-192 (14), and with *N*-(1-oxyl-2,2,6,6-tetramethyl-4-piperidinyl)-*m*-fluorosulfonylbenzamide (SL-2), which specifically sulfonylates Ser-195 (15). SL-2 was synthesized as described (16), and chymotrypsin was spin labeled with each spin label according to published procedures (17).

The spin-labeled enzyme was immobilized at pH 7.0 to controlled-pore glass (Sigma; 75 Å nominal pore size) by rotoevaporation from either 0.01 M sodium phosphate buffer, pH 7.0 (SL-2), or 1 mM acetic acid adjusted to pH 7.0 with dilute NaOH (SL-1). The immobilized enzyme was then dried at room temperature for 24 hr at 10 millitorr (1.3 Pa) and transferred to organic solvents for EPR analysis at 25°C on a Bruker ER200D-SRC EPR spectrometer (microwave power, 12.6 mW; modulation amplitude, 1.0 G; scan range, 150 G). All organic solvents were dried initially over molecular sieves and contained 0.01–0.02% (wt/wt) water, as measured by Karl-Fischer titration. Immobilized enzyme was used in all experiments to prevent aggregation of the insoluble enzyme in organic solvents.

The spectral simulations are based on a Brownian rotational diffusion model for axially symmetric diffusion (18). The simulated spectra were generated by systematically varying the label's two rotational correlation times, $\tau_\parallel$ and $\tau_\perp$, to minimize the least-squares difference between the calculated and experimental spectra. The A and g values required for the simulation of room-temperature spectra were determined from rigid-limit simulations of EPR spectra recorded at 120 K. The best fits between theoretical and experimental spectra were obtained by assuming that $\tau_\parallel$ corresponds to rotation about an axis parallel to the $2p\pi$ orbital of the nitrogen and $\tau_\perp$ corresponds to rotation about axes perpendicular to it.

MD simulations were performed by using a modified version of AMBER 3.0 (19). Details of the protein MD algo-

Abbreviations: MD, molecular dynamics; SL-1 (spin label 1), *N*-(1-oxyl-2,2,6,6-tetramethyl-4-piperidinyl)iodoacetamide; SL-2 (spin label 2), *N*-(1-oxyl-2,2,6,6-tetramethyl-4-piperidinyl)-*m*-fluorosulfonylbenzamide.

*To whom reprint requests should be addressed.

rithm are described elsewhere (20). The program was expanded to account for the local dielectric constant throughout the protein, which was modeled in several ways. Results reported here were obtained with the microdielectric model (8). The motions of all protein atoms were included explicitly and the solvent was modeled as a continuum with stochastic properties. The initial protein configuration used to obtain the equilibrium structure in the continuum was the crystal structure of α-chymotrypsin determined by Tsukada and Blow (21). Calculations were performed for chymotrypsin in an ionization state corresponding to pH 7.0, and surface charges were kept ionized at all values of ϵ. The MD calculations consisted of 50 psec of equilibration at 298 K and a 100- to 150-psec equilibrium simulation. The equilibrated structure at one dielectric constant (e.g., 5) was used as the initial structure at the next higher dielectric constant (e.g., 7). The mean squared errors for calculated correlation times were less than ±1.5 psec in all simulations. Similar trends were obtained when the effective dielectric constant model (22) and the Kirkwood–Westheimer–Tanford model were used (23). Color images were generated by using BIOGRAF software on a TITEN Graphics Supercomputer.

RESULTS

Shown in Fig. 1 are the experimental and simulated EPR spectra of spin-labeled α-chymotrypsin in various nearly dry organic solvents. A convenient indicator of the spin label's overall motion is the mean rotational correlation time of the nitroxide, τ_R. The mean rotational correlation time is defined as $\tau_R = (\tau_\parallel \tau_\perp)^{1/2}$. For each spin-labeled amino acid, τ_R decreased with increasing solvent dielectric constant, ϵ (Fig. 2). The results are best described by τ_R (nsec) = $76\epsilon^{-0.67}$ for Met-192 and τ_R (nsec) = $30\epsilon^{-0.77}$ for Ser-195. A preliminary analysis based on linear self-consistent field theory (24) suggests that the leading coefficients of these power-law expressions are residue-specific parameters sensitive to the concentration and orientation of charged groups surrounding the amino acid. No such dependence of the spin label's motion on solvent dielectric was observed for the free spin label dissolved in organic solvents, suggesting that the spectra of Fig. 1 reflect changes in the local dynamics of the enzyme. Specifically, it appears that motions of the protein in the vicinity of the spin-labeled residues are strongly influenced by the dielectric constant of the solvent.

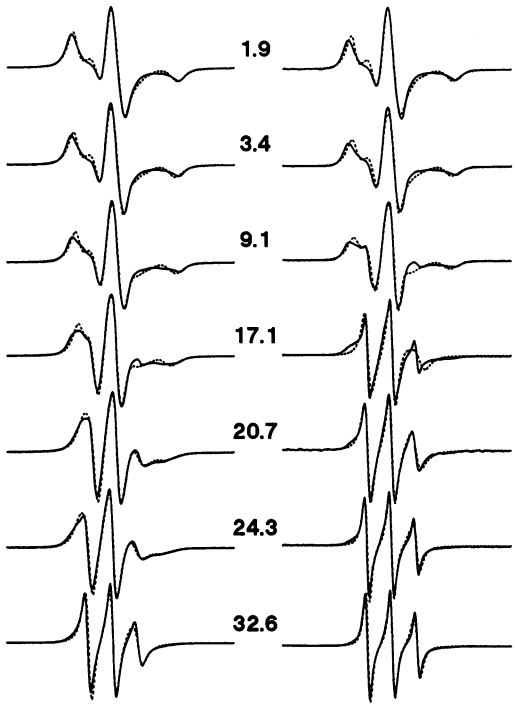

FIG. 1. Experimental (solid lines) and simulated (broken lines) EPR spectra of immobilized chymotrypsin spin-labeled at Met-192 with SL-1 (*Left*) and at Ser-195 with SL-2 (*Right*). The simulated spectra were generated as described in the text and are independent of the MD simulations. Experimental spectra were recorded in nearly anhydrous organic solvents of different dielectric constants, listed in the center. Solvents, from top: hexane, trichloroethylene, methylene chloride, butanol, acetone, ethanol, and methanol.

Brooks *et al.* (25) point out that the solvent viscosity can influence the dynamics of some atoms in proteins, particularly those exposed to solvent, without having much effect on others. In the case of spin-labeled chymotrypsin, there was no correlation between motion and solvent viscosity for either spin label. Nor did spin-label motion correlate with the

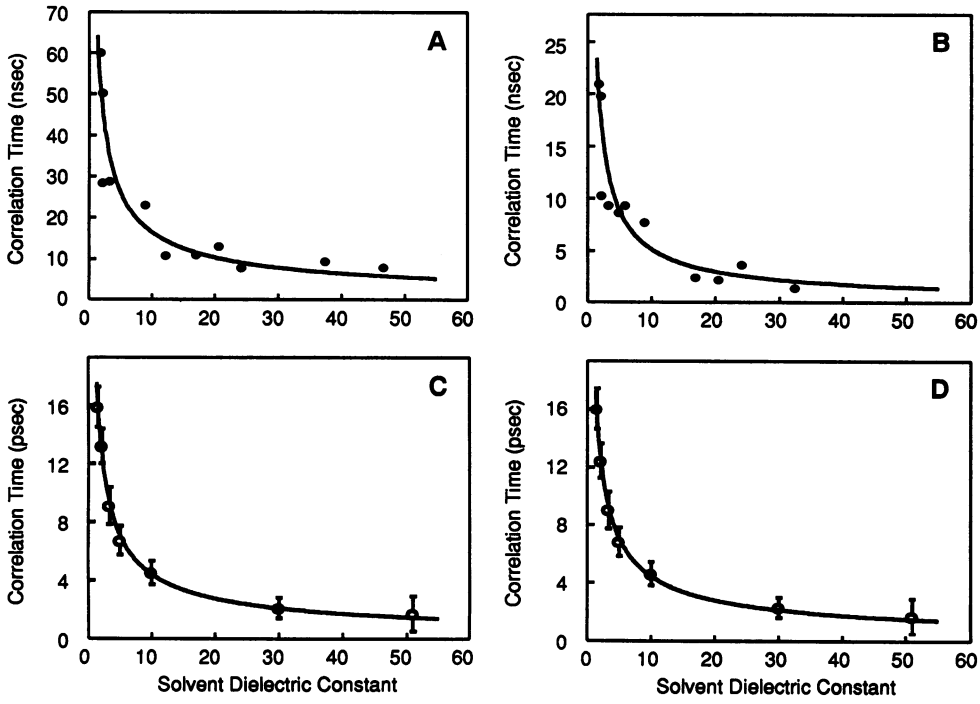

FIG. 2. Rotational correlation times of enzyme-bound spin labels determined from spectral simulations of EPR spectra (*A* and *B*), and correlation times of α-carbon atoms determined from MD simulations (*C* and *D*). (*A*) Spin-labeled Met-192. (*B*) Spin-labeled Ser-195. (*C*) C^α of Met-192. (*D*) C^α of Ser-195. The solid lines represent curve fits of the data, as described in the text. The mean squared errors for the calculated correlation times are shown by the error bars in *C* and *D*. Solvents and dielectric constants: hexane (1.89), carbon tetrachloride (2.24), benzene (2.28), trichloroethylene (3.40), butyl acetate (5.01), ethyl acetate (6.02), methylene chloride (9.08), pyridine (12.3), butanol (17.1), acetone (20.7), ethanol (24.3), methanol (32.6), acetonitrile (37.5), and dimethyl sulfoxide (46.7).

diffusivities of water in the organic solvents calculated from a modified Wilke–Chang correlation (26). For each organic solvent, the diffusion constant of water was regarded as a possible measure of mobility for the limited amount of water near the protein.

To determine whether a simple model of electrostatic interactions could reproduce the essential features of the EPR data, we have modeled charged groups on the protein as point charges on the ends of mechanical springs. For example, to describe the electrostatic interaction between Asp-102 and His-57 in the enzyme's active site, the negatively charged aspartic residue (i) is treated as a point charge rigidly bound to the polypeptide backbone of the protein. The positive charge on the histidine residue (j) is modeled as a point charge attached to the backbone through a flexible chain characterized by a Hookian spring constant k. The potential energy function, $\Gamma_{ij}(x)$, characterizing interactions between residues i and j is then given by

$$\Gamma_{ij}(x) = \Gamma(x)^{\text{Hooke}} + \Gamma(x)^{\text{elec}} = \frac{1}{2}kx^2 + \frac{z_i z_j e^2}{\epsilon(x - x')}, \quad [1]$$

where x is the position of the oscillating charge, x' is the position of the fixed charge, z_i is the valence of residue i, e is the electronic charge, and ϵ is the dielectric constant of the fluid between the two charges. Minimization of the potential energy function around the equilibrium position of residue j gives a second-order harmonic differential equation in $\Gamma_{ij}(x)$ with a characteristic vibrational frequency ν of

$$\nu = \frac{1}{2\pi\sqrt{m_j}}\left(k + \frac{2z_i z_j e^2}{\epsilon x'^3}\right)^{1/2}, \quad [2]$$

where m_j is the mass of residue j. Eq. 2 indicates that vibrational frequencies of oppositely charged residues increase with increasing solvent dielectric constant as a result of changes in the electrostatic force between the residues. A dependence of atomic fluctuations on solvent dielectric constant is consistent with the EPR measurements and spectral simulations of spin-labeled chymotrypsin and with previously reported, albeit qualitative, spin-labeling studies of horse liver alcohol dehydrogenase (27).

A more complete representation of dielectric effects on protein dynamics has been provided by MD simulations, in which dipole–dipole, dipole–induced-dipole, and electrostatic interactions are all considered. MD results for Met-192 and Ser-195 are shown in Fig. 2, along with the rotational correlation times of each spin-labeled amino acid determined from EPR measurements and spectral simulations. The correlation time obtained from MD simulations is the time interval between successive displacements (of mean distance greater than 1.1 Å) of a protein atom from its original, average position. The correlation times shown in Fig. 2 *C* and *D* apply to the α-carbon atoms of Met-192 and Ser-195, respectively. The theoretical results are τ_R (psec) = $21\epsilon^{-0.68}$ for Met-192 and τ_R (psec) = $21\epsilon^{-0.67}$ for Ser-195.

The MD calculations and EPR results exhibit good agreement in their power-law dependence on the solvent dielectric constant; however, the predicted motions of the backbone atoms are notably faster than the measured motions of the nitroxide spin labels. This difference could be due to several

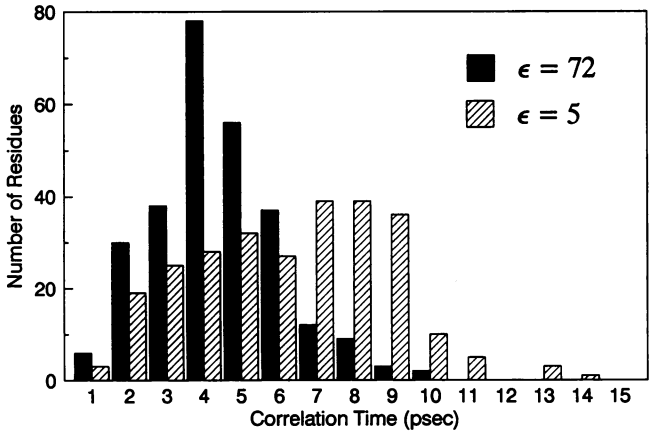

FIG. 3. Histograms of correlation times of α-carbon atoms of chymotrypsin calculated for solvent dielectric constants of 5 and 72 at 298 K.

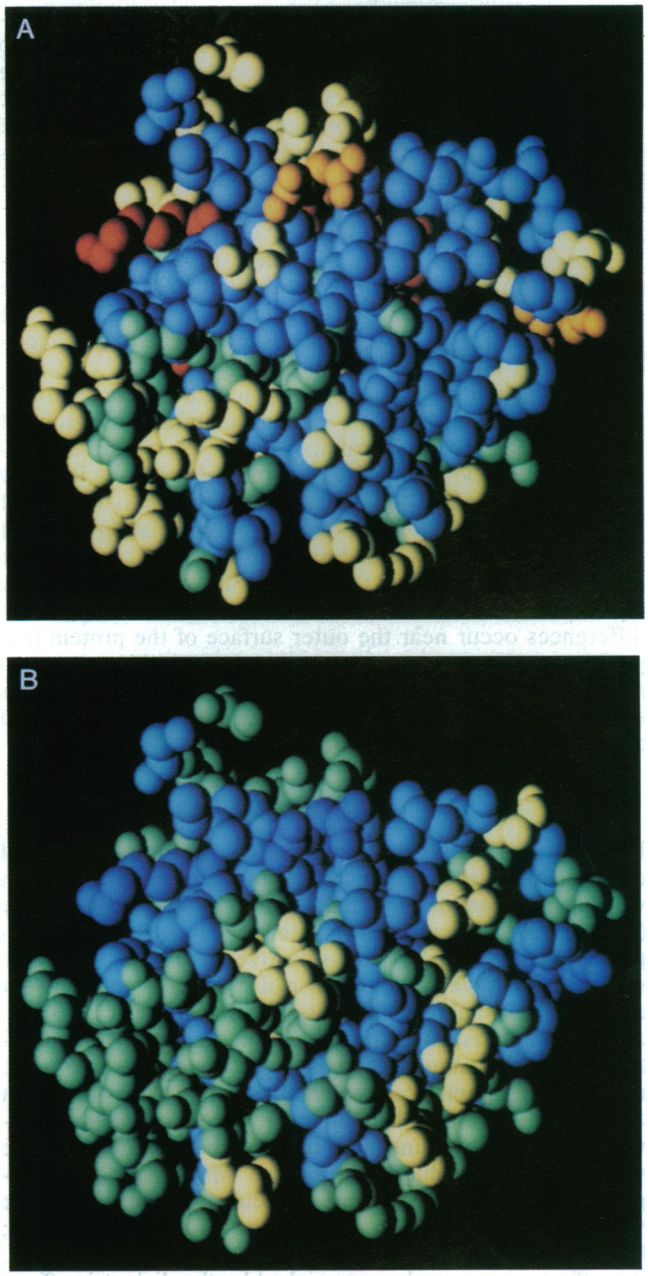

FIG. 4. Cutaway cross-sections of chymotrypsin molecule, showing correlation times of individual residues at dielectric constants of 5 (*A*) and 72 (*B*). Correlation times are color coded as follows: dark blue, 0–2.5 psec; light blue, 2.5–5.0 psec; green, 5.0–7.5 psec; yellow, 7.5–10 psec; orange, 10–12.5 psec; and dark orange, 12.5–15 psec. The residues shown define the cross-section at a radial distance of 25 Å from Leu-10 on the surface of the protein. The active site is located near the lower left edge.

factors, including intrinsic limitations in the accuracy of the calculations and/or the spectral simulations. Moreover, the molecular motion of the nitroxide ring at the end of the spin label is expected to be slower than the motion of the α-carbon atom due to the additional degrees of freedom introduced by the intervening chemical bonds and to hindrance by neighboring residues of the protein. Therefore the nanosecond time scale of the nitroxide motions most likely corresponds more closely to side-chain motions of amino acids, which, in polycrystalline form, have been shown by NMR relaxation measurements to have correlation times of $\approx 10^{-8}$ sec (28). Nonetheless, the EPR results and MD simulations reveal a very similar functional dependence between the rates of motion in the protein and the dielectric constant of the bulk solvent.

Further insights into the effects of solvent dielectric constant are provided by the histograms of Fig. 3. The two histograms compare the calculated correlation times of all the α-carbon atoms of chymotrypsin for continuum dielectric constants of 72 and 5. At the higher dielectric constant, the distribution of relaxation times is fairly symmetric and is centered at a value of about 4 psec. At the lower dielectric constant, the mean has shifted to about 6 psec, the distribution is much broader, and there is a large grouping in the 6- to 9-psec range. Further, the range of correlation times spanned by atoms of the protein is about 30% greater at the lower dielectric constant. These calculations suggest that the change of dielectric slows some atoms of the enzyme molecule but has little effect on others.

Because polar or ionizable groups tend to be concentrated near the protein surface, we expect the influence of solvent to be strongest at the protein–solvent interface. This expected tendency is consistent with the color-coded MD results shown in Fig. 4. The two cutaway cross-sections of the chymotrypsin molecule depict the correlation times of individual residues at dielectric constants of 72 and 5. The distribution of motions throughout the protein is clearly different for the two cases. In general, the most significant differences occur near the outer surface of the protein (the periphery of each cross-section), where residues tend to move more slowly for $\epsilon = 5$. Thus, the picture that emerges at $\epsilon = 5$ is of a protein with a more rapidly moving core and a more slowly moving exterior.

CONCLUDING REMARKS

Enzymes in nearly dry organic solvents can exhibit novel catalytic properties compared with their counterparts in water—for example, markedly different enantioselectivity (29). The kinetic parameters of enzymatic reactions in organic solvents can be very sensitive to the nature of the solvent, and in the particular case of subtilisin, to the solvent dielectric constant (29). In addition to the dielectric constant, other characteristics of the solvent no doubt play an important role in determining the properties of proteins in organic media. For example, Zaks and Klibanov (30) have shown that chymotrypsin retains less bound water in hydrophilic solvents such as pyridine and acetone than in hydrophobic solvents such as toluene and octane. More extensive stripping of water from the enzyme molecule by more hydrophilic solvents might serve to rigidify the protein (4, 13, 31); however, for the chymotrypsin samples under present study, this effect appears to be outweighed by the dielectric effect, since protein motions are faster in the more hydrophilic (higher ϵ) solvents. In particular, our spin-labeling experiments and MD simulations show that many motions in chymotrypsin, and presumably in other proteins as well, become more rapid with increasing solvent dielectric constant. Nonaqueous solvents should therefore prove useful for examining possible relationships between the dynamics and functions of proteins.

We thank D. Chandler for many helpful discussions, and we are grateful to A. Warshel, J. F. Kirsch, H. W. Blanch, and J. M. Prausnitz for helpful comments. This work was supported by the National Science Foundation Presidential Young Investigator Award of D.S.C. and by the Army Research Office (DAAL03-91-G-0224). R.A. and C.A.H. were partially supported by a National Institutes of Health training grant. We also acknowledge the use of the University of California, San Francisco, Computer Graphics Lab, supported by National Institutes of Health Division of Research Resources Grant RR-1081, R. Langridge, Principal Investigator, to visualize the protein structures.

1. Wüthrich, K. (1989) *Science* **243**, 45–50.
2. Ringe, D. & Petsko, G. A. (1985) *Prog. Biophys. Mol. Biol.* **45**, 197–235.
3. Cusack, S., Smith, J., Finney, J., Tidor, B. & Karplus, M. (1988) *J. Mol. Biol.* **202**, 903–908.
4. Bone, S. (1987) *Biochim. Biophys. Acta* **916**, 128–134.
5. Karplus, M. & Petsko, G. A. (1990) *Nature (London)* **347**, 631–639.
6. McCammon, J. A. & Harvey, S. C. (1987) *Dynamics of Proteins and Nucleic Acids* (Cambridge Univ. Press, Cambridge).
7. Perutz, M. F. (1978) *Science* **201**, 1187–1191.
8. Warshel, A. & Russell, S. T. (1984) *Q. Rev. Biophys.* **17**, 283–422.
9. Rogers, N. K. (1986) *Prog. Biophys. Mol. Biol.* **48**, 37–66.
10. Zaks, A. & Klibanov, A. M. (1984) *Science* **224**, 1249–1251.
11. Dordick, J. S. (1989) *Enzyme Microb. Technol.* **11**, 194–211.
12. Randolph, T. W., Clark, D. S., Blanch, H. W. & Prausnitz, J. M. (1988) *Science* **239**, 387–390.
13. Rupley, J. A., Yang, P. H. & Tollin, G. (1980) *ACS Symp. Ser.* **127**, 111–132.
14. Kosman, D. J. & Piette, L. H. (1972) *Arch. Biochem. Biophys.* **149**, 452–460.
15. Berliner, L. J. & Wong, S. S. (1974) *J. Biol. Chem.* **249**, 1668–1677.
16. Wong, S. S., Quiggle, K., Triplett, C. & Berliner, L. J. (1974) *J. Biol. Chem.* **249**, 1678–1682.
17. Bailey, J. E. & Clark, D. S. (1987) *Methods Enzymol.* **135**, 502–512.
18. Freed, J. H. (1976) in *Spin Labeling: Theory and Applications*, ed. Berliner, L. J. (Academic, New York), pp. 53–132.
19. Weiner, S. J., Kollman, P. A., Case, D. A., Singh, U. C., Ghio, C., Alagona, G., Profeta, S., Jr., & Weiner, P. (1984) *J. Am. Chem. Soc.* **106**, 765–784.
20. Weiner, P. K. & Kollman, P. A. (1981) *J. Comp. Chem.* **2**, 287–303.
21. Tsukada, H. & Blow, D. M. (1985) *J. Mol. Biol.* **184**, 703–711.
22. Davis, M. E. & McCammon, J. A. (1990) *Chem. Rev.* **90**, 509–521.
23. Tanford, C. & Kirkwood, J. G. (1957) *J. Am. Chem. Soc.* **79**, 5333–5339.
24. Chandler, D. (1987) *Introduction to Modern Statistical Mechanics* (Oxford Univ. Press, New York).
25. Brooks, C. L., III, Karplus, M. & Pettitt, B. M. (1988) *Proteins: A Theoretical Perspective of Dynamics, Structure, and Thermodynamics* (Wiley, New York), pp. 33–59.
26. Olander, D. R. (1961) *AIChE J.* **7**, 175–176.
27. Guinn, R. M., Skerker, P. S., Kavanaugh, P. & Clark, D. S. (1991) *Biotechnol. Bioeng.* **37**, 303–308.
28. Andrew, E. R., Hinshaw, W. S., Hutchins, M. G. & Sjöblom, R. O. I. (1977) *Mol. Phys.* **34**, 1695–1706.
29. Fitzpatrick, P. A. & Klibanov, A. M. (1991) *J. Am. Chem. Soc.* **113**, 3166–3171.
30. Zaks, A. & Klibanov, A. M. (1988) *J. Biol. Chem.* **263**, 3194–3201.
31. Affleck, R., Xu, Z.-F., Suzawa, V., Focht, K., Clark, D. S. & Dordick, J. S. (1992) *Proc. Natl. Acad. Sci. USA* **89**, 1100–1104.